ISSN 2321-807X
Volume 12 Number15
Journal of Advances in chemistry

Structural and spectral studies on benzoyl Thiourea based on DFT calculations

Dr.R.Kumutha[1], Dr.S.Sampath Krishnan*[2] Rubarani.P.Gangadharan[3] and M.Thirumalai Kumar
[1]Department of Physics, S.A Engineering College, Chennai
kumuthar@saec.ac.in
[2]Department of Applied Physics, Sri Venkateswara College of Engineering,
Sriperumbudur- 602105 , India
sambathk@svce.ac.in
[3]Department of Physics, Rajalakshmi Engineering College,Thandalam,Chennai-602105
rubarani.p.gangadharan@rajalakshmi.edu.in
[4]Department of Applied Chemistry, Sri Venkateswara College of Engineering,
Sriperumbudur-602 105, India
mtkumar@svce.ac.in
*Corresponding author e-mail: sambathk@svce.ac.in Tel:9444245284

ABSTRACT

The experimental and theoretical vibrational spectra of benzoyl thiourea were investigated. The experimental FT-IR (400–4000 cm−1) and FT-Raman spectra (100–4000 cm−1) of the molecule in the powder form were recorded. Theoretical vibrational frequencies and geometric parameters (bond lengths and bond angles) were calculated using density functional B3LYP method with 6-311G++(d,p) and cc-pVDZ basis sets by Gaussian program, for the first time. The complete assignments were performed on the basis of the potential energy distribution (PED) of the vibrational modes, calculated with scaled quantum mechanical (SQM) method. The formation of the hydrogen bond was investigated using NBO calculations. The electron density-based local reactivity descriptors such as Fukui functions were calculated. The calculated HOMO and LUMO energies show that charge transfer occur within the molecule. The dipole moment (μ) and polarizability (α), anisotropy polarizability ($\Delta\alpha$) and first order hyperpolarizability (βtotal) of the molecule have been reported

Indexing terms/Keywords

FTIR, FT-Raman, DFT, NBO

Academic Discipline And Sub-Disciplines

Applied Physics

SUBJECT CLASSIFICATION

Physics Subject Classification; Spectroscopy

TYPE (METHOD/

Quantum Chemical Calculation – DFT studies

INTRODUCTION

A number Thiourea derivatives and their transition metal complexes have been known since the beginning of the 20th century. The syntheses of the thiourea derivatives are easily with good yields. Thiourea and its derivatives represent a well-known important group of organic compounds due to diverse application in the field of such as medicine, agriculture, coordination, and analytical chemistry. The benzoyl thiourea have a wide range of biological activities including antiviral, antibacterial, antifungal, ant-tubercular, herbicide ,insecticidal , pharmacological properties and to act as chelating agents. Thiourea and its derivatives have been becoming increasingly important in research and technological application such as inhibitors in the corrosion field[1,2]. The inhibition of corrosion in acidic medium has been previously studied by numerous researchers using different organic compounds[3,4] due to thiourea derivatives ability to minimize corrosion effect on various metals. The effectiveness of this organic compound is believed to be due to the presence of lone pair of electrons in atom such as nitrogen, N, sulphur, S and oxygen, O, and π- electron cloud that are capable of forming dative covalent bond with metals[5,6]. Literature survey reveals that to the best of our knowledge, the results based on quantum chemical calculations, vibrational spectral studies and HOMO–LUMO analyses on benzoyl thiourea have no reports. In this study molecular geometry, optimized parameters and vibrational frequencies are computed and the performances of the computational methods for B3LYP at 6-31G (d, p) basis sets are compared. These methods predict relatively accurate molecular structure and vibrational spectra with moderate computational effort. In particular for polyatomic molecules the DFT methods lead to the prediction of more accurate molecular structure and vibrational frequencies than the conventional ab initio Hartree–Fock calculations. Among DFT calculation, Beck's three Parameter hybrids functional combined with the Lee–Yang–Parr correlation functional (B3LYP) is the best predicting results for molecular geometry and vibrational wave numbers for moderately larger molecule[7, 8].

EXPERIMENTAL DETAILS

The fine polycrystalline of benzoyl thiourea was purchased from Sigma–Aldrich Chemical Company with a stated purity 97% and it was used as such without further purification. The FTIR spectrum of molecule was recorded in the region 450–4000 cm−1 on a Perkin Elmer FTIR BX spectrometer calibrated using polystyrene bands. FT-Raman spectrum of the sample was recorded using 1064 nm line of Nd:YAG laser as excitation wave length in the region 1000–5000 cm−1 on a Bruker RFS 100/S FT-Raman spectrometer. Liquid nitrogen cooled Gediode was used as a detector. Spectra were collected for samples with 1000 scan accumulated for over 30 min duration.. A correction according to the fourth power scattering factor was performed, but no instrumental correction was done.

COMPUTATIONAL DETAILS

In order to obtain stable structures, the geometrical parameters of in the ground state was optimized at DFT-B3LYP level of theory using 6-311++G(d,p) and cc-pVDZ basis sest. There are no significant differences between geometric and vibrational frequencies by the selection of the different basis sets. The calculated vibrational frequencies are scaled by 0.967 for B3LYP/6-311++G(d,p) [9]. For B3LYP with cc-pVDZ basis set, the wave numbers in the ranges from 4000 to 100 cm−1 are scaled with 0.970 [10]. The molecular geometry was not restricted and all the calculations (vibrational wave numbers, geometric parameters and other molecular properties) were performed by using Gauss View molecular visualization program [11].

,All calculations were carried out with the Gaussian 03 package [12]. The calculations of systems contain C,H, N,O and S is described by the standard 6-311++G(d, p) and cc-pVDZ basis sets function of the density functional theory(DFT) [13,14]. Geometry optimization was performed utilizing Becker's hybrid three-parameter exchange functional and the nonlocal correlation functional of Lee, Yang and Parr (B3LYP) [15]. Vibrational analysis was performed at each stationary point found, that confirm its identity as an energy minimum. The population analysis has also been performed by the natural bond orbital method [16] at B3LYP/6-311++G(d,p) level of theory using NBO program [17] under Gaussian 03 program package

RESULTS AND DISCUSSION

Geometric structure

The fourier

The molecular structure of benzoyl thiourea belongs to Cs point group symmetry. The optimized molecular structure of title molecule is obtained from Gaussian 03 program. The labeling of atoms in is given in Fig.1. The optimized geometrical parameters (bond lengths and angles) calculated by B3LYP with 6-311G++(d,p) and cc-pVDZ basis sets are listed in Table 1.The calculated C-C bond length of the ring varied such as C5-C6,C6-C7,C6-C11,C7-C8,C8-C9,C9-C10,C10-C11. But the bond length of C9-C10 and N1-C2 well coincides, calculated by B3LYP method with 6-31G++(d,p) and cc-pVDZ basis sets. The N4-H16 bond distance is very small compared than all other bond lengths and N4-C7 is very large compared to all other bond lengths of the title molecule. The bond lengths determined from B3LYP method with 6-311++G (d,p) basis set is slightly lower than that obtained from other methods.The density functional calculation gives the very high bond angle of C2-N1-C5 (147°).The C-C-H angle is constant which is found to be 120◦ of this compound. The electron donating substituents on the benzene ring, the symmetry of the ring is distorted, yielding ring angles smaller than 120◦ at the point of substitution and slightly larger than 120◦ at the ortho and Meta positions [18].The N4-C7-C6 bond gives very small angle 92.7◦ .The variation in bond angle depends on the electro negativity of the central atom, the presence of lone pair of electrons and the conjugation of the double bonds. If the electro negativity of the central atom decreases ,the bond angle decreases. Further the results of our calculations, the experimental and calculated geometric parameters agree well with remaining geometrical parameters. The small deviations observed are probably due to the intermolecular interactions in the crystalline state of the molecule .

ISSN 2321-807X
Volume 12 Number15
Journal of Advances in chemistry

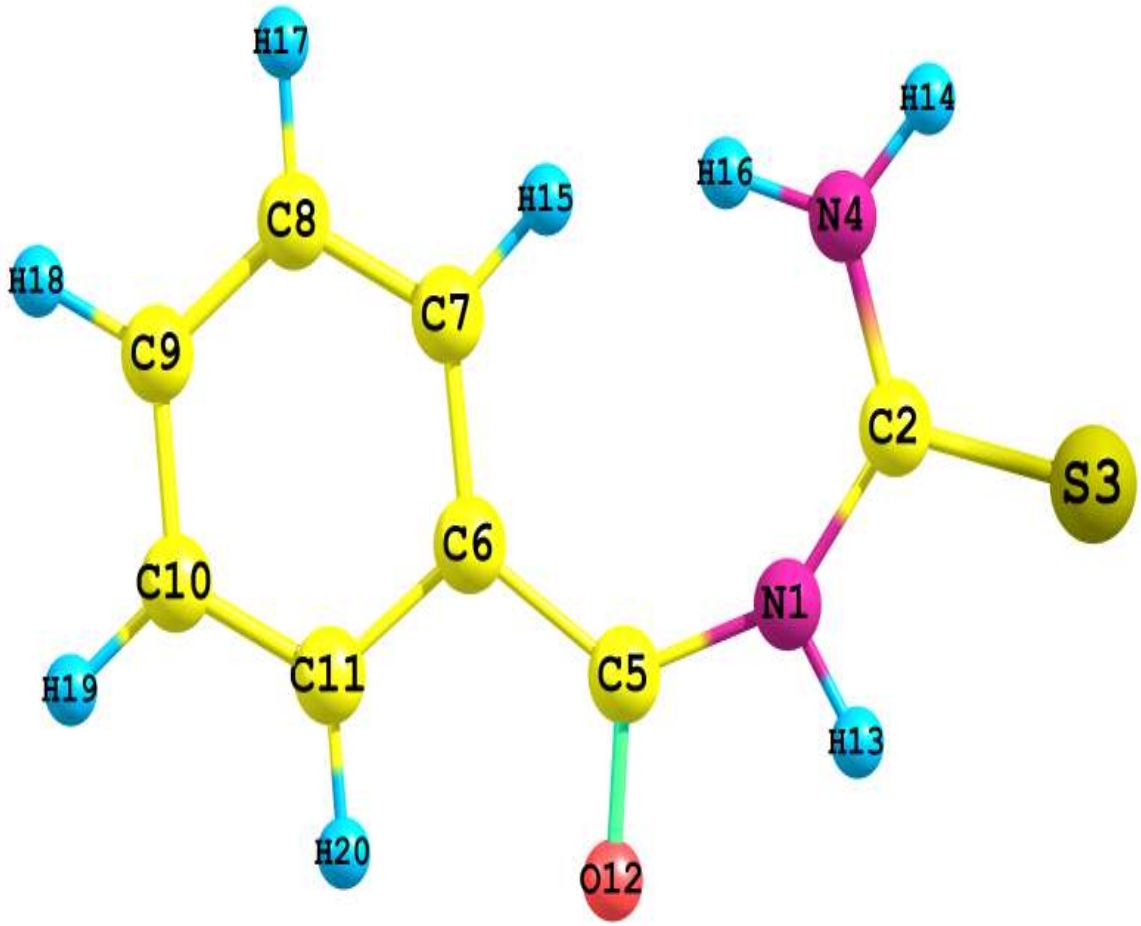

Figure 1 The atom numbering system for benzoyl thiourea

Table 1 Optimized geometric parameters of benzoyl thiourea by B3LYP/6-311++G and B3LYP/cc-pVDZ methods

Parameter	Method/basis set		
Bond length(Å)	B3LYP/ 6-311++G(d,p)	B3LYP/ cc-pVDZ	Experimental*
N(1)-C(2)	1.393	1.393	1.399
N(1)-C(5)	1.423	1.421	1.4 27
N(1)-H(13)	1.015	1.020	1.018
C(2)-S(3)	1.677	1.685	1.655
C(2)-N(4)	1.345	1.345	1.354
N(4)-C(7)	3.323	3.331	3.073
N(4)-H(15)	2.456	2.453	2.357
N(4)-H(16)	1.004	1.005	1.009
C(5)-C(6)	1.514	1.515	1.499
C(5)-O(12)	1.219	1.224	1.119
C(6)-C(7)	1.399	1.403	1.402
C(6)-C(11)	1.409	1.413	1.393

C(7)-C(8)	1.394	1.397	1.385
C(7)-H(15)	1.074	1.083	1.087
C(7)-H(16)	2.463	2.476	2.401
C(8)-C(9)	1.39	1.395	1.339
C(8)-H(17)	1.084	1.092	1.104
C(9)-C(10)	1.394	1.394	1.395
C(9)-H(18)	1.084	1.092	1.054
C(10)-C(11)	1.388	1.392	1.338
C(10)-H(19)	1.084	1.092	1.054
C(11)-H(20)	1.081	1.088	.1.087
H(15)-H(16)	1.499	1.498	1.397
Bond Angle(°)			
C (2)-N(1)-C(5)	147.831	147.858	147.5
C(2)-N(1)-H(13)	107.395	107.214	108.2
C(5)-N(1)-H(13)	104.774	104.928	104.7
N(1)-C(2)-S(3)	117.728	117.445	117.3
N(1)-C(2)-N(4)	121.598	122.123	122
S(3)-C(2)-N(4)	120.674	120.432	120
C(2)-N(4)-C(7)	98.474	98.019	98
C(2)-N(4)-H(14)	116.667	116.078	116
C(2)-N(4)-H(15)	111.182	110.745	110
C(2)-N(4)-H(16)	124.404	124.792	124.3
C(7)-N(4)-H(14)	144.859	145.903	145
H(14)-N(4)-H(15)	132.151	133.176	133
H(14)-N(4)-H(16)	118.929	119.129	188.8
N(1)-C(5)-C(6)	129.502	129.321	130
N(1)-C(5)-O(12)	112.684	112.85	112.5
C(6)-C(5)-O(12)	117.814	117.824	--
C(5)-C(6)-C(7)	129.817	129.937	129.1
C(5)-C(6)-C(11)	113.199	113.067	113.2
C(7)-C(6)-C(11)	116.98	116.996	117.2
N(4)-C(7)-C(6)	92.777	92.742	93.12
N(4)-C(7)-C(8)	145.636	145.682	--
C(6)-C(7)-C(8)	121.586	121.576	122.3
C(6)-C(7)-H(15)	122.973	122.694	121.5
C(6)-C(7)-H(16)	103.007	103.279	103
C(8)-C(7)-H(15)	115.441	115.729	115
C(8)-C(7)-H(16)	135.406	135.145	134.2
C(7)-C(8)-C(9)	120.394	120.411	120
C(7)-C(8)-H(17)	119.283	119.253	119.9

C(9)-C(8)-H(17)	**120.322**	**120.337**	**120**
C(8)-C(9)-C(10)	**119.109**	**119.087**	**119**
C(8)-C(9)-H(18)	**120.317**	**120.316**	**124**
C(10)-C(9)-H(18)	**120.574**	**120.597**	**120**
C(9)-C(10)-C(11)	**120.272**	**120.249**	**--**
C(9)-C(10)-H(19)	**120.263**	**120.259**	**--**
C(11)-C(10)-H(19)	**119.465**	**119.493**	**119.2**
C(6)-C(11)-C(10)	**121.655**	**121.682**	**--**
C(6)-C(11)-H(20)	**117.989**	**117.644**	**118.3**
C(10)-C(11)-H(20)	**120.356**	**120.674**	**120.5**

VIBRATIONAL ANALYSIS

The vibrational spectral assignments of benzoyl thiourea have been carried out with the help of PED analysis. The internal coordinates describe the position of the atoms in terms of distances, angles with respect to an origin atom. In this study, the full sets of 70 standard internal coordinates for title compound were defined as given in Table 2. The experimental FT-IR and FT-Raman spectra are shown in Figs. 2 and 4, respectively. For a comparative purpose the calculated IR and Raman spectra with 6-311G++ (d,p) basis sets are shown in Figs 3 and 5, respectively. The scaled calculated harmonic vibrational frequencies at B3LYP levels, observed vibrational frequencies and detailed PED assignments are tabulated in Table 3. To our knowledge, there are no theoretical studies on the vibrational assignments of benzoyl thiourea in the literature. So , in order to introduce detailed vibrational assignments of benzoyl thiourea. We have performed computational analysis done by using PED analysis and the visualization of modes.

Table 2 Definition of internal coordinates of benzoyl thiourea

No.	Type	Definition
Stretching		
1-7	C-C	C5-C6,C6-C7,C6-C11, C7-C8,C8-C9,C9-C10, C10-C11
8-12	C-H	C7-H15,C8-H17,C9-H18,C10-H19,C11-H20
13-15	C-N	N1-C2,N1-C5, C2-N4
16-18	N-H	N1-H13,N4-H14, N4-H16
19	C-S	C2-S3
20	C-O	C5-O12
In-Plane Bending		
21-26	Ring	C6-C7-C8,C7-C8-C9,C8-C9-C10,C9-C10-C11, C6-C11-C10, C7-C6-C11
27-28	C-N-C	C2-N1-C5,N1-C5-C6
29-38	C-C-H	C6-C7-H15,C6-C11-H20,C8-C7-H15,C7-C8-H17, C9-C8-H17, C8-C9-H18, C10-C9-H18, C9-C10-H19, C11-C10-H19, C10-C11-H20
39	C-C-O	C6-C5-O12
40-41	C-C-C	C5-C6-C7, C5-C6-C11
42-45	C-N-H	C2-N1-H13, C5-N1-H13, C2-N4-H14, C2-N4- H16
46-47	N-C-S	N1-C2-S3, S3-C2-N4

48	N-C-N	N1-C2-N4
49	N-C-O	N1-C5-O12
50	H-N-H	H14-N4-H16
Out-of-Plane bending		
51-57	C-H	H19-C10-C11-C9,H18-C9-C10-C8,H17-C8-C9-C7,H20-C11-C6-C10, H15-C7-C8-C6, H16-N4-C2-H14,H14-N4-H16-C2
58-60	C-N	S3-C2-N4-N1,O12-C5-N1-C6,H13-N1-C2-C5
Torsion		
61-66	τ ring	C10-C11-C6-C7, C11-C6-C7-C8, C6-C7-C8-C9, ,C7-C8-C9-C10, C8-C9-C10-C11, C9-C10-C11-C6
67-68	Butterfly 1	C8-C7-C6-C5,H15-C7-C6-C11
69-70	Butterfly 2	H16-N4-C2-O3,H14-N4-C2-N1

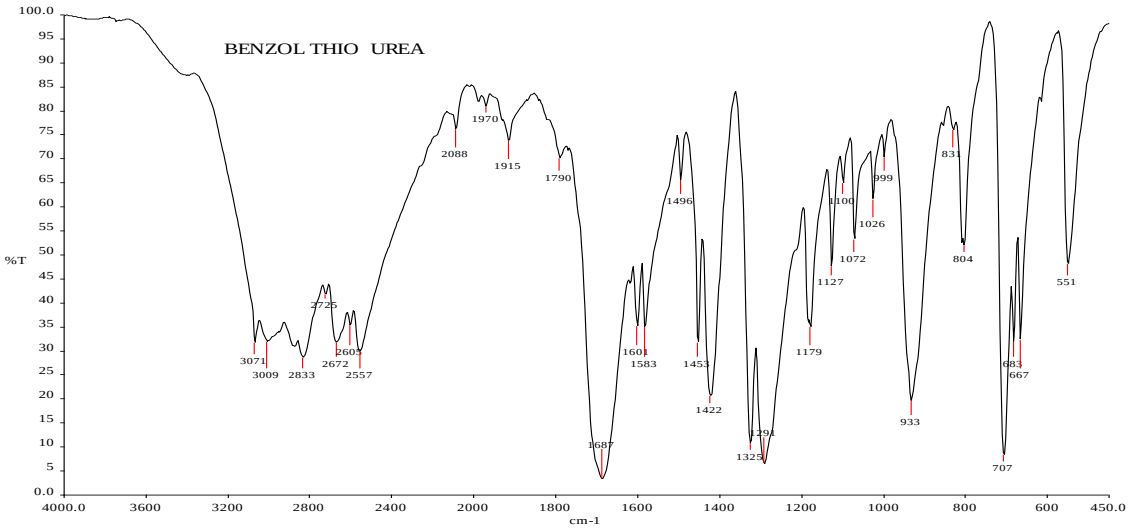

Figure 2 The experimental FT-IR spectrum of title molecule

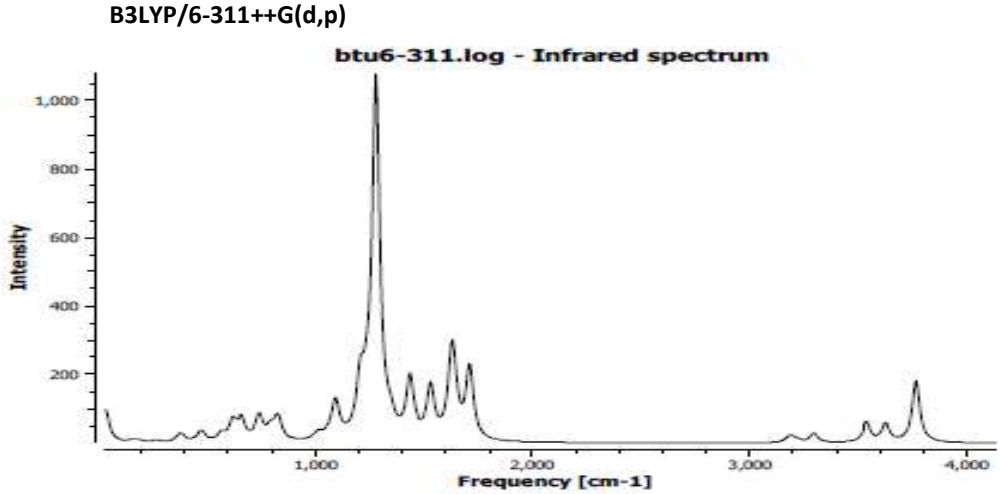

Figure 3 Comparative graph of calculated IR spectra

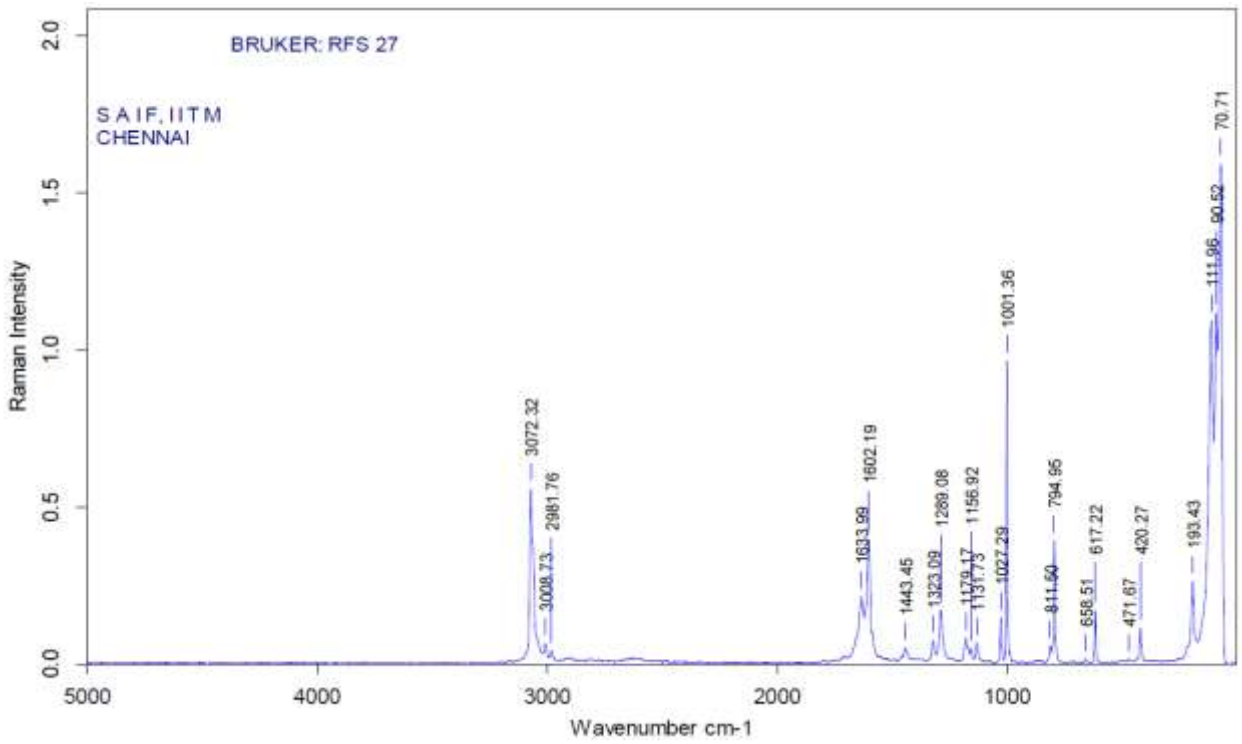

Figure 4 The experimental FT-Raman spectrum of title molecule

B3LYP/6-311++G(d,p)

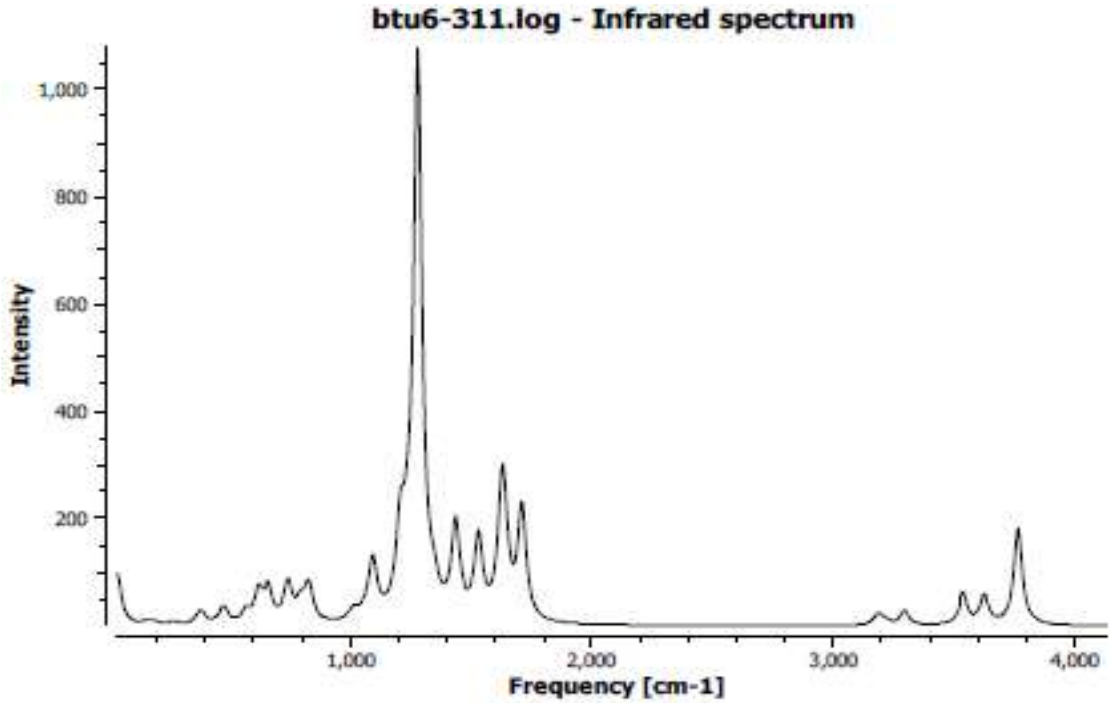

Fig. 5. Comparative graph of calculated FT-Raman spectrum.

Table 3 The observed FT-IR, FT-Raman and calculated wave numbers using B3LYP method with 6-311++G(d,p) and cc-pVDZ basis sets and probable assignments for benzoyl thiourea

Mode No	Observed frequencies(cm-1)		Calculated frequencies(cm-1)				Vibrational assignments (>10%PED)
	FT-IR	FT-Raman	B3LYP/6-311++G(d,p)		B3LYP/cc-pVDZ		
			Unscaled	Scaled	Unscaled	Scaled	
1	3450(w)	---	3464	3425	3454	3451	vasNH2 (70),vsNH2 (30)
2	---	3320(vw)	3326	3313	3305	3303	vsNH2 (69),vasNH2(30)
3	3243(w)	---	3238	3208	3226	3209	vsNH (100)
4	---	3197(vw)	3296	3187	3303	3203	vsC7H15 (98)
5	3127(w)	----	3224	3117	3239	3141	vsC11H20 (99)
6	---	3100(vw)	3194	3088	3204	3107	vsC10H19 (98)
7	3071(s)	3072(vs)	3182	3076	3191	3095	vsC8H17(98)
8	3009(w)	3008(vw)	3172	3067	3181	3085	vs C9H18(97)
9	1790(w)	1633(w)	1710	1653	1724	1672	vsOC(74)
10	1687(vs)	1602(vs)	1643	1588	1653	1603	vsC10C11(50),vsN1C5(37)
11	1583(vs)	1567(vw)	1616	1562	1613	1564	vC6C7(47),vsC10C11(24)
12	1496(s)	---	1533	1482	1519	1473	vsC9C8(85)
13	1453(s)	1439(vw)	1521	1470	1507	1461	vsC9C10(70),vsC9C8(25)
14	1422(s)	1427(vw)	1469	1420	1467	1422	vsC8C7(44),vsC10C11(20),sN4C2(21)
15	1351(vs)	---	1329	1315	1409	1380	vsN4C2(51),vsN1C2(36)
16	---	1343(w)	1383	1345	1381	1337	vsN1C2(79)
17	1325(vs)	1323(vw)	1346	1301	1363	1322	vN1C5(72)
18	1291(w)	1389(s)	1328	1284	1317	1277	vC11C6(52),vsCS(22)
19	1240(vw)	---	1279	1236	1294	1255	vCSsym(67)
20	---	1203(vw)	1238	1197	1244	1206	βC11C6C7 (39),βH15C6C7(27),τHNCN(10)
21	1179(s)	---	1208	1168	1196	1160	βNH2(72),vC6C7(27)
22	1127(s)	1179(w)	1187	1147	1174	1138	βH18N4C2(68),vsC9C10(29)
23	1100(s)	1156(vw)	1125	1087	1123	1089	βH14N4C2(48),βC11C6C7 (29),βC9C8C7(12)
24	1072(vs)	1070(vw)	1095	1058	1099	1066	βH15C6C7(42),vC11C6(22),βNH2(17)
25	1026(vs)	1027(s)	1056	1021	1058	1026	βH17C8C9(35),βNH2(27),βH18N4C21(68)
26	999(w)	1001(vs)	1022	988	1031	1000	βH19C10C9(43),βH14N4C2(28),vsC8C7(24)
27	---	990(vw)	1014	980	1017	986	βH15C8C7(42),vsC9C8(25),vC11C6(22)
28	980(vw)	---	1010	976	1009	978	βH17C8C7(40),vC11C6(22),ωC10C8C9(17)
29	---	959(vw)	992	959	999	969	γO12C5N1(38),τHCCC(22),τHCCC(17)
30	933(vs)	--	914	883	924	896	γN1C2N4(29) ,τHNCC(25),ωC10C8C9(18)
31	831(vw)	811(vw)	828	800	832	807	γC9C8C7(37),βH15C8C7(25),butt(18)
32	804(s)	--	816	789	830	805	ωC10C8C9(39),C2-N1def(10),τHNCN(22)
33	---	794(s)	794	767	816	791	ωC8C7C6(34),βH17C8C7(24),Rdef(12)
34	712V(w)	---	743	718	784	760	ωC2N1C5(33),Butt(23)
35	707(vs)	---	724	700	724	702	βN1C5C6(27),Rdef(18)
36	683(s)	---	672	649	682	661	γC9C10C11(31),Rasymdef(26)
37	667(s)	658(vw)	661	639	664	644	βS2C2N4(37),τONCC(30),ω(12)

38	---	617(w)	635	614	631	612	τH16N4C2N1(79)
39	601(vw)	---	617	596	616	597	γC9C8C7(36),τH13N1C5C6(22)
40	---	583(vw)	597	577	607	588	τH14N4C2N1 (80),τHCCC(10)
41	551(s)	----	565	546	565	548	τH20C10C11C6(23),N1C2C4 adef(22)
42		471(vw)	476	460	513	497	τHCCC(80)
43	----	460(vw)	467	451	468	453	τHCCC(32),vsC8C7(24)
44	----	420(w)	433	418	443	429	γH18C8C9C10(42),τH20C11C6C7(21)
45	380(vw)	---	389	376	390	378	Rdif (32),γasydefH16N4C2N1(19)
46	370(w)	---	377	364	387	375	τHCCC(37),as.def C10-C11
47	282(vw)	---	269	260	269	260	τCCCC (49),Rdef(32)
48	193(w)	---	184	177	185	179	butt(38),βS2C2N4(17)
49	----	---	162	156	161	156	butt(29),τHCCC(18)
50	111(vs)	---	148	143	155	150	butt(22),γC9C8C7(17)
51	90(vs)	---	60	58	80	77	Rtwist(36),NH2adef(21)
52	---	---	41	39	39	38	τONCC (29),τring(18)
53	---	---	49	37	37	36	τSNNC(28),βC11C6C7 (19)
54	---	---	35	33	35	32	τC5–O12 (25),τC5–N1(15)

Abbreviations: s-strong; vs-very strong ;ms-medium strong; w- weak ;vw-very weak; ν-stretching; β- in plane bending; γ-out 0f plane bending ω- wagging; τ-Torsion.,def-deformation, Butt-butterfly , Rdef. Ring deformation, Rasymdef- Ring asymmetric deformation, Wag-wagging

COMPUTED IR INTENSITY AND RAMAN ACTIVITY ANALYSIS

Computed vibrational spectral IR intensities and Raman activities of the title compound by DFT method with B3LYP at 6-311++G (d, p) and cc-pVDZ basis sets have been collected in Table 4. The title molecule is a non polar and belongs to CS point group. Comparison of IR intensity and Raman activity are calculated by B3LYP with 6-311++G (d, p) and cc-pVDZ basis sets. In the case of IR intensity the values by B3LYP/6-311++G(d,p) are found to be higher than B3LYP at cc-pVDZ levels.

Table 4 Comparative values of IR intensity and Raman activity between B3LYP/6-311++G(d,p) and B3LYP/cc-pVDZ of benzoyl thiourea

Mode no	Calculated value		Calculated value	
	B3lyp/6-311++g(d,p)		B3lyp/cc-pvdz	
	Air intensity	Bramanintensity	Air intensity	Braman intensity
1	37.7	0.2	30.0	1.3
2	3.5	0.7	2.2	1.1
3	0.1	0.3	0.0	0.4
4	0.2	0.5	0.0	0.6
5	1.9	1.3	1.6	2.1
6	0.1	0.5	0.1	0.5
7	2.6	0.4	3.1	0.5
8	2.3	1.7	2.4	1.7
9	7.9	0.1	7.1	0.0
10	3.9	0.6	4.4	0.8
11	0.5	0.0	0.6	0.1
12	2.0	0.8	1.6	0.9
13	11.8	0.1	26.1	1.1

14	9.7	3.3	11.6	2.7
15	0.1	1.0	0.1	2.6
16	23.6	4.1	20.7	3.9
17	2.6	2.9	2.6	2.5
18	25.9	0.1	17.5	0.3
19	1.5	0.1	0.9	0.4
20	0.5	2.3	0.2	1.7
21	31.0	0.3	6.1	0.5
22	14.0	0.0	16.2	1.0
23	2.1	0.2	13.7	0.5
24	28.3	11.5	21.8	5.7
25	0.1	0.0	0.0	0.8
26	0.4	0.0	0.2	0.0
27	4.8	11.1	4.8	2.6
28	3.5	10.4	1.4	10.1
29	0.1	0.0	0.0	0.1
30	6.9	12.0	4.9	10.3
31	47.3	1.8	24.6	1.1
32	0.3	1.2	0.5	2.0
33	0.1	2.6	0.1	3.1
34	63.7	5.4	38.6	2.0
35	29.3	18.1	3.1	7.7
36	45.2	62.0	38.4	43.9
37	2.9	0.9	50.3	8.4
38	14.8	7.0	7.5	2.0
39	74.2	22.2	59.9	24.9
40	2.8	5.2	1.4	1.3
41	2.9	4.3	66.1	20.9
42	62.2	45.1	5.3	8.4
43	2.4	1.8	100.0	2.1
44	100.0	44.1	22.2	11.4
45	26.8	21.3	1.7	41.4
46	90.7	58.4	81.6	53.0
47	0.1	24.6	0.1	26.5
48	3.9	43.8	4.5	46.2
49	6.2	100.0	7.2	100.0
50	2.2	31.1	1.9	30.3
51	11.8	49.8	13.3	53.0
52	26.1	18.9	28.3	17.9
53	23.2	70.9	21.2	66.4
54	77.7	60.1	73.0	57.3

a Relative absorption intensities normalized with highest peak absorption equal to 100.

b Relative Raman activities normalized to 100.

CH STRETCHING VIBRATIONS

The existence of one or more aromatic rings in a structure is normally readily determined from the C–H and C–C ring related vibrations. The substituted benzene like molecule gives rise to C–H stretching, C–H in-plane and C–H out-of-plane bending vibrations. The hetro aromatic structure shows the presence of C–H stretching vibration in the region 3100–3000 cm−1, which is the characteristic region for the ready identification of C–H stretching vibration [19,20]. In this region, the bands are not affected appreciably by the nature of the substituent. The aromatic C − H stretching frequencies arise from the modes observed at 3062, 3047 cm−1and 3080 cm−1 of benzene and its derivatives [21]. In our present work, the C–H stretching vibrations are observed at 3127, 3071 and 3009 cm−1in FT-IR and at 3197, 3100cm−1in FT-Raman spectrum. The calculated values of these modes for the title molecule have been found to be 3187,3117,3088,3076 and 3067 cm−1 at B3LYP calculation level. As indicated by the PED, these five modes involve approximately 99% contribution suggesting that they are pure stretching modes.

CH BENDING VIBRATIONS

The aromatic C–H in-plane bending modes of benzene and its derivatives are observed in the region 1300–1000 cm−1 [22]. The C-H in plane bending vibrations are identified at 1179, 1127,1100,1072,1026, 999 and 990 cm−1in FT-IR and at 1203, 1179, 1156,1027,1001 and990 cm−1 in FT-Raman spectrum. The aromatic C–H in-plane bending vibrations have substantial overlapping with the ring C–C stretching vibrations. The absorption bands arising from C–H out-of-plane bending vibrations are usually observed in the region at 1000–675 cm−1 [23]. The C–H out-of-plane bending vibrations are observed as strong bands in FTIR at 993, 831, 804, 7712 cm−1 and Raman active mode can be observed as medium bands in Raman spectrum at 811, 794 cm−1. The HCH, HCC bending vibrations are observed in both spectra with 45% of PED contribution. This also shows good agreement with theoretically scaled harmonic wave number values.

CC VIBRATIONS

The carbon–carbon stretching modes of the phenyl group are expected in the range from 1650 to 1200 cm−1. The actual position of these modes is determined not so much by the nature of the substituents but by the form of substitution around the ring. In general, the bands are of variable intensity and are observed at 1625–1590, 1590–1575, 1540–1470, 1465–1430 and 1380–1280 cm−1 from the wave number ranges given by Varsanyi[24] for the five bands in the region. In the Present work, the wave numbers observed in the FTIR spectrum at 1687, 1610, 1583,1496,1453,1422 cm−1 in FT-IR spectrum and in FT- Raman spectrum at 1567, 1439, 1427 cm−1 have been assigned to C–C stretching vibrations. The theoretically computed values at 1588, 1515,1562,1482,1470 and 1420, cm−1 show an excellent agreement with experimental data. These modes are mixed mode with the contribution of C–H in-plane bending vibration in this region, and the modes are confirmed by the PED values as shown in Table 3.

The aromatic C–C in-plane bending modes of benzene and its derivatives are observed in the region 1300–1000 cm−1.The C–C–C out-of-plane bending modes are observed at 683,601cm−1and these wave numbers are consistent with the theoretical wave numbers. The same vibrations are predicted for benzoyl thiourea at 649 and 596cm−1 by B3LYP methods. The C–C–C in-plane and out-of-plane bending vibrations are also computed theoretically and the correlation between the experimental and theoretical values are observed.

CN VIBRATIONS

In aromatic compounds, the C-N stretching vibrations usually in the region 1400–1200 cm−1. The identification of CN stretching frequencies was a rather difficult task since the mixing of vibrations was possible in this region [25, 26]. In this study, the bands observed at 1351 and 1325cm−1 in FT-IR spectrum and 1343 and 1323 cm−1 in Raman spectrum have been assigned to CN stretching vibrations of the title compound. The in-plane and out-of plane bending CN vibrations had also been identified and presented in Table 4.

C=O STRETCHING

The band due to C=O stretching vibration is observed in the region 1850-1550 cm−1 due to tautomerism, pyrimidine's substituted with hydroxyl groups are generally in the keto form and therefore, have a strong band due to carbonyl group. In the present work, the bands observed at 1790 cm−1 in FTIR spectrum and 1633 cm−1 (mode no. 09) in Raman are assigned to C=O stretching mode of vibrations

NH2 Vibration

The calculated NH2 asymmetric stretching vibrations give rise to the strong band at 3639,3641 cm-1 compare with the experimental result at 3650 cm-1. The theoretical observed NH2 symmetric stretching vibration give rise to the strong band at 3506,3496 cm-1 compare with the experimental value at 3520 cm-1. Heteroaromatics containing an N-H group show their stretching vibrations in the region 3500-3220 cm-1. The position of the absorption in this region depends upon the degree of hydrogen bonding and hence, upon the physical state of the sample or the polarity of the solvent. In the present work, the bands appearing at 3443cm-1 in the FTIR (mode no3). The theoretical observed NH symmetric stretching vibration give rise to 3421 and 3420 cm-1.

C–H BENDING C–

The C–H deformation frequencies in benzene and its derivatives are found to occur in the region 1200-1000 cm−1. In the present work the bands observed at 1072 cm−1 and 1026 cm−1 (mode nos. 24 and 25) in FTIR spectrum and the bands at 1070 and 1027 cm−1 in FT Raman spectrum of benzoyl thiourea are assigned to C–C–H symmetric and asymmetric bending, respectively.

NBO ANALYSIS

NBO analysis provides an efficient method for studying intra and intermolecular bonding and interaction among bonds, and also provides a convenient basis for investigation charge transfer or conjugative interactions in molecular system [27].Some electron donor orbital, acceptor orbital and the interacting stabilization energy resulting from the second order micro-disturbance theory are reported [28,29] .The larger the E(2) value, the more intensive is the interaction between electron donors and the greater the extent of conjugation of the whole system. Delocalization of electron density between occupied Lewis type(bond or lone pair) NBO orbitals and formally unoccupied (antibonding or Rydberg) non Lewis NBO orbital's correspond to a stabling donor-acceptor interaction. NBO analysis performed on the molecule at the DFT/B3LYP/6-31++1G(d,p) level in order to elucidate the intra molecular rehybridization and delocalization of electron density within the molecule. The molecular interaction is formed by the orbital overlap between σ(C-C) and σ*(C-C) bond orbital which results intramolecular charge (ICT) causing stabilization of the system. These interactions are observed as increase in electron density(ED) in C-C antibonding orbital that weakens the respective bonds. The electron density of conjugated double as well as the single bond of the conjugated ring (~1.9 e) clearly demonstrates strong delocalization inside the molecule.

Natural bond orbital analysis stresses the role of intermolecular orbital interaction in the complex, particularly charge transfer. This is carried out by considering all possible interactions between filled donor and empty acceptor NBOs and estimating their energetic importance by second-order perturbation theory. For each donor NBO(i) and acceptor NBO (j), the stabilization energy E(2) associated with electron delocalization between donor and acceptor is estimated as:

$$E(2) = q_i \frac{(F_{i,j})^2}{\varepsilon_j - \varepsilon_i}$$

Where qi is the orbital occupancy, εi, εj are diagonal elements and Fi,j is the off-diagonal NBO Fock matrix element.

Table 5 Second order perturbation theory analysis of fock matrix in nbo basis in benzoyl thiourea

Donor(i)	Type	ED(e)	Acceptor(j)	Type	ED(e)	E(2)a (kJ/mol)	E(j)-E(i)b (a.u.)	F(i,j)c (a.u.)
N1-C2	Σ	1.9869	C5-O12	σ*	0.0149	2.57	1.51	0.056
			N4-H14	σ*	0.0365	1.78	1.18	0.041
N1-C5	Σ	1.9864	C5-C6	σ*	0.0604	2.92	1.22	0.053
N1-H13	Σ	1.9832	C2-N4	σ*	0.0861	4.71	1.09	0.065
C2-S3	Π	1.9815	C2-S3	π*	0.3954	4.23	0.25	0.032
C2-N4	Σ	1.9535	C7-H15	σ*	0.0820	28.55	3.05	0.266
			N4-H16	σ*	0.0851	133.94	3.86	0.648
N4-H14	Σ	1.9448	N1-C2	σ*	0.0644	2.64	1.10	0.048
			C2-N4	σ*	0.0861	3.39	1.09	0.048
			N4-H16	σ*	0.0851	176.75	3.74	0.731
			N4-H14	σ*	0.0365	41.68	2.93	0.314
N4-H16	σ	1.9289	C7-C8	σ*	0.0463	5.29	2.23	0.097
			C7-H15	σ*	0.0820	2.73	3.84	0.092
			N4-H16	σ*	0.0851	20.85	4.65	0.279
C5-C6	σ	1.9681	C6-C7	σ*	0.0563	4.17	1.36	0.068
			C6-C11	σ*	0.0316	5.63	1.40	0.079
C5-O12	σ	1.9720	C5-C6	σ*	0.0604	3.97	1.68	0.074
			C6-C7	π*	04520	7.08	0.41	0.054

C6-C7	σ	1.9314	N4-H16	σ*	0.0851	19.16	3.73	0.240
			C7-C8	σ*	0.0462	10.50	1.31	0.105
			C7-H15	σ*	0.0820	98.22	2.92	0.480
	π	1.6163	C5-O12	π*	0.0149	33.34	0.30	0.091
			C8-C9	π*	0.0214	17.43	0.32	0.068
C6-C11	σ	1.9658	C10-C11	π*	0.0188	30.32	4.86	0.036
C6-C7				σ*	0.0563	7.06	1.34	0.086
C7-C8	σ	1.9333	C7-H15	σ*	0.0820	91.27	4.40	0.093
C6-C7				π*	0.4520	24.62	0.30	0.079
C10-C11	σ	1.9748	C10-C11	π*	0.2779	16.02	4.86	0.267
C6-C7				π*	0.4520	24.62	0.30	0.079
C10-C11	σ	1.9748	C10-C11	π*	0.2779	16.02	4.86	0.267
C10-H19				σ*	0.1842	29.26	4.05	0.308
C11-H20	σ	1.9743	C10-C11	π*	0.2779	49.95	4.62	0.459
C10-H19				σ*	0.0184	18.70	3.81	0.239
N1	LP(1)	1.6198	C2-S3	π*	0.3954	65.56	0.22	0.108

ED Electron Density

a E(2) means energy of hyper conjugative interaction (stabilization energy).

b Energy difference between donor and acceptor i and j NBO orbitals.

c F(i,j) is the Fock matrix element between i and j NBO orbitals.

In Table 5 the perturbation energies of donor-acceptor interactions are presented. In our title molecule benzoyl thiourea π(C6-C7) →π*(C5-O12) has 33.34 kJ/mol, π(C8-C9) →π*(C6-C7) has 24.62 kJ/mol and σ(N4-H14) → σ*(N4-H14)has 41.68 kJ/mol and hence they give stronger stabilization to the structure. From the Table-5 it is noted that the maximum occupancies 1.9869, 1.9864, 1.9832, 1.9815 are obtained for σ(N1-C2), σ(N1-C5), σ(N1-H13) and π((C2-S3) respectively. Therefore the results suggest that the σ(N1-C2), σ(N1-C5), σ(N1-H13) and π((C2-S3) are essentially controlled by the p-character of the hybrid orbital's.

The same kind of interaction is calculated in the same kind of interaction energy, related to the resonance in the molecule, is electron donating from σ (N1-C2) to σ* (N4-H14) shows less stabilization of 1.78 kJ/mol and σ (C2-N4) to σ* (N4-H16) further leads to strong stabilization energy of 133.94 kJ/mol and σ(N4-H14) to σ*(N4-H16) resulting in an enormous stabilization of 176.75 kJ/mol. The strong intra-molecular hyper conjugation interaction of the σ and the π electrons of C-C to the anti C-C bond in the ring leads to stabilization of some part of the ring as evident from the Table- 5.

FRONTIER MOLECULAR ORBITAL ANALYSIS

The HOMO (highest occupied molecular orbital)–LUMO (lowest unoccupied molecular orbital) energy gap of hydroxybenzopyridine has been calculated at the B3LYP/6-311++G(d,p). Many organic molecules containing π conjugated electrons are characterized hyperpolarizabilities and were analyzed by means of vibrational spectroscopy [30,31]. These orbitals determine the way the molecule interacts with other species. Fig. 6 shows the distributions and energy levels of the HOMO−1, HOMO, LUMO and LUMO+1 orbitals computed at the B3LYP/6-311++G(d,p) level for the title compound. The calculated energy values are presented in Table 6. HOMO is mainly localized on the hydroxyl group and LUMO is delocalized over the entire molecule. HOMO−1 is delocalized over the entire molecule and LUMO+1 is localized on the hydroxyl group and methyl group. The value of the energy separation between the HOMO and LUMO is 0.15313 a.u. The lowering of the HOMO–LUMO band gap is essentially a consequence of the large stabilization of the LUMO due to the strong electron-acceptor ability of the electron-acceptor group. The higher the energy of HOMO, the easier it is for HOMO to donate electrons whereas it is easier for LUMO to accept electrons when the energy of LUMO is low. Moreover lower in the HOMO–LUMO energy gap explains the eventual charge transfer interactions taking place within the molecule

Table 6 HOMO–LUMO energy value of BTU calculated by B3LYP method with 6-311++G (d,p) and cc-pVDZ basis sets

Parameters	B3lyp/6-311++g(d,p) (ev)	B3lyp/cc-pvdz (ev)
EHOMO	-6.2129	-5.8004
ELUMO	-2.4221	-2.0835
ΔE(HOMO-LUMO) gap	3.7908	3.7467
EHOMO-1	-6.4720	-6.1008
ELUMO+1	-1.2650	-0.9143
ΔE(HOMO-1-LUMO+1)gap	5.2069	5.1865

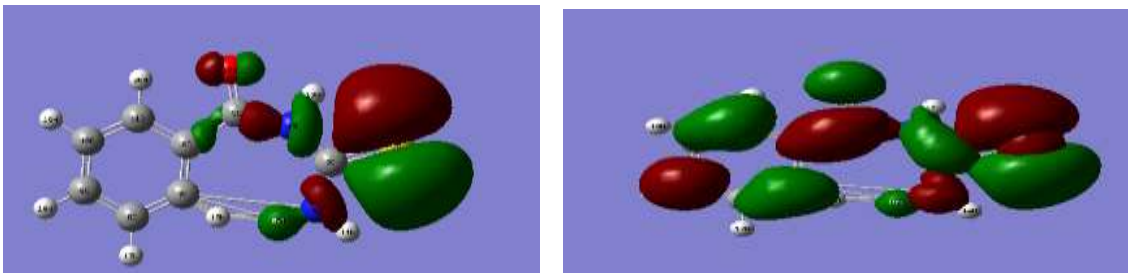

HOMO **LUMO**

Fig 6. The atomic orbital composition of the frontier molecular orbital of benzoyl thiourea

Mulliken Atomic charges

Mulliken atomic charges calculation has an important role in the application of quantum chemical calculation to molecular system because atomic charges affect dipole moment, molecular polarizability, electronic structure and a lot of properties of molecular systems [32]. The charge distribution over the atoms suggests the formation of donor and acceptor pairs involving the charge transfer in the molecule. Atomic charge has been used to describe the processes of electro -negativity equalization and charge transfer in chemical reactions [33,34]. Mulliken atomic charges calculated by methods B3LYP/6-311++G(d,p) and B3LYP/cc-pVDZ methods are collected in Table -7. It is worthy to mention that C2,C5,C7 and C11 atoms of the title molecule exhibit positive charge while C6,C8,C9 and C10 atoms exhibit negative charges. Sulphur has a maximum negative charge value of about -0.810. The maximum positive atomic is obtained for C7 which is a carbon present in the CH functional group. The charge on H13 in the functional group has the maximum magnitude of 0.366 among the hydrogen atoms present in the molecule at 6-311++G(d,p) level of theory. However all the hydrogen atoms exhibit a net positive charge in 6-311++G(d,p) basis set except H15. The presence of large negative charge on O and N atom and net positive charge on H atom may suggest the formation of intermolecular interaction in solid forms [35].

Table 7 Mulliken Atomic Charges Calculated By B3lyp/6-311++G (D,P) And B3lyp/Cc-Pvdz Methods

Atoms	B3LYP/ 6-311++G(d,p)	B3LYP/ cc-pVDZ	Atoms	B3LYP/ 6-311++G(d,p)	B3LYP/ cc-pVDZ
N1	-0.019	-0.093	C11	-0.010	0.087
C2	0.143	0.056	O12	-0.261	-0.226
S3	-0.579	-0.286	H13	0.344	0.126
N4	-0.397	-0.008	H14	0.299	0.122
C5	0.415	-0.175	H15	-0.112	-0.056
C6	1.032	-0.045	H16	0.397	0.059
C7	-0.402	0.016	H17	0.197	-0.025
C8	-0.045	0.045	H18	0.166	-0.016
C9	-0.134	0.049	H19	0.182	-0.014
C10	-0.512	0.046	H20	0.227	-0.010

OTHER MOLECULAR PROPERTIES

Analysis of molecular electrostatic potential (MESP)

Molecular electrostatic potential (MEP) at a point in the space around a molecule gives an indication of the net electrostatic effect produced at that point by the total charge distribution (electron + nuclei) of the molecule and correlates with dipole moments, electronegativity, partial charges and chemical reactivity of the molecules [36,37]. It provides a visual method to understand the relative polarity of the molecule. The different values of the electrostatic potential represented by different colors; red represents the regions of the most negative electrostatic potential, white represents the regions of the most positive electrostatic potential and blue represents the region of zero potential. Potential increases in the order red < green < blue < pink < white. It can be seen that the negative regions are mainly over the O12 atom. The negative (red color) regions of MEP were related to electrophilic reactivity and the positive (white color) ones to nucleophilic reactivity. The negative electrostatic potential corresponds to an attraction of the proton by the aggregate electron density in the molecule (shades of red), while the positive electrostatic potential corresponds to the repulsion of the proton by the atomic nuclei (shades of white) According to these calculated results, the MEP map shows that the negative potential sites are on oxygen atoms as well as the positive potential sites are around the hydrogen atoms. These sites give information concerning the region from where the compound can have metallic bonding and intermolecular interactions. The predominance of light green region in the MESP surfaces corresponds to a potential halfway between the two extremes red and dark blue co lour. The total electron density and MESP surfaces of the molecules under investigation are constructed by using B3LYP/6–31G (d,p) method. These pictures illustrate an electrostatic potential model of the compounds, computed at the 0.002 a.u. isodensity surface. The MEP mapped surface of the compounds and electrostatic potential map for positive and negative potentials is shown in Fig7. The MEP map shows that the negative potential sites are on electronegative atoms as well as the positive potential sites are around the hydrogen atoms. These sites give information about the region from where the compound can have non covalent interactions.

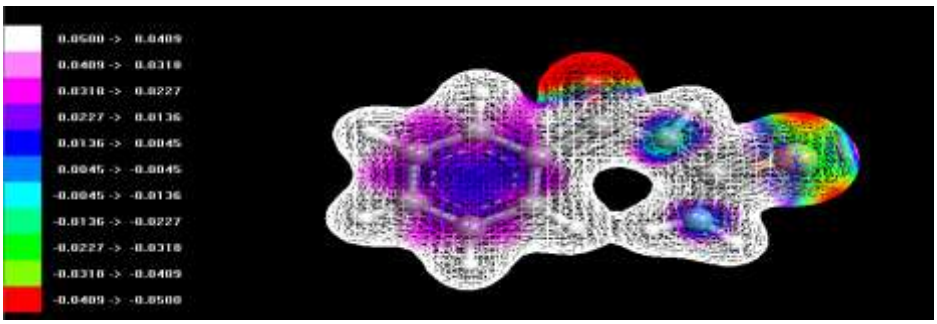

Fig 7 Molecular electrostatic potential map of benzoyl thiourea

First order hyperpolarizability calculations

Polarizabilities and hyperpolarizabilities characterize the response of a system in an applied electric field[38]. They determine not only the strength of molecular interactions as well as the cross sections of different scattering and collision processes, but also the non-linear optical properties (NLO) of the system [39,40].In order to investigate the relationships among photocurrent generation, molecular structures and NLO, the Polarizabilities and hyperpolarizabilities of title compound was calculated using B3LYP method, 6-311++G(d,p) basis set, based on the finite-field approach. The first order hyperpolarizability (β) of title molecule along with related properties (μ, α, and $\alpha o_{,}$) are reported in Table- 8. The calculated value of dipole moment was found to be 1.5839 Debye at B3LYP/6-311++G(d,p). In addition to the isotropic Polarizabilities and Polarizabilities anisotropy invariant were also calculated. The calculated anisotropy of the polarizability $\alpha_{,}$ of benzoyl thiourea is 293.268 a.u at B3LYP/6-311++G(d,p) level. The magnitude of the molecular hyperpolarizability β, is one of key factors in a NLO (non-linear optical) system. The B3LYP/6-31G(d,p) calculated first order hyperpolarizability value (β0) of benzoyl thiourea is equal to 2.3720 x 10−30 esu. Total dipole moment of title molecule is slightly smaller than those of urea and first order hyperpolarizability of title molecule is approximately eight times greater than those of urea. This result indicates the nonlinearity of the title molecule.

Table 8 the b3lyp/6-311++g(d, p) calculated electric dipole moments (debye), polarizability (in a.u.), β components and βtot (10−31 esu) value of benzoyl thiourea

parameters	b3lyp/6-31++g (d,p)	parameters	b3lyp/ 6-311++g(d,p)
μx	-1.5647	β xxx	339.816
μy	-0.2444	β xxy	-159.355
μz	0	β xyy	-211.601
μ	1.5839	β yyy	-53.574

α xx	159.6619	βxxz	0.0707
αxy	-26.9998	β xyz	-0.0195
αyy	165.3166	βyyz	-0.0235
α xz	0	β xzz	-24.8076
α yz	0	β yzz	-41.4093
α zz	64.9899	β zzz	0
α0	129.989	βtot (esu)	2.3720 x 10−30
α	293.268		

FUKUI FUNCTIONS

DFT is one of the important tools of quantum chemistry to understand popular chemical concepts such as electro negativity, electron affinity, chemical potential and ionization potential. In order to solve the negative Fukui function problem, different attempts have been made by various groups [41]. Kolandaivel et al.[42] introduced the atomic descriptor to determine the local reactive sites of the molecular system. In the present study, the optimized molecular geometry was utilized in single-point energy calculations, which have been performed at the DFT for the anions and cat ions of the title compound using the ground state with doublet multiplicity. The individual atomic charges calculated by natural population analysis (NPA) and Mulliken population analysis (MPA) have been used to calculate the Fukui function. Table -9 shows the fk+, fk-2 and fk0 values for the title molecule calculated by NPA and MPA gross charges at DFT level of theory with the basis set (B3LYP/6-311++G(d,p)). It has been found that both NPA and MPA scheme methods predict that the sulphur atom S3 has a higher fk+ value for nucleophilic attack. Also both the population analysis schemes show N4 nitrogen atom as the reactive sites for receiving a nucleophilic . From the values reported in the Table -9 the reactivity order for the electrophilic case was C9>C8>C5 for MPA analysis. On the other hand for nucleophilic attack both S3 and C2 has greater reactivity value. The attack for radical case was S3>H15 for MPA. If one compares the three kinds of attacks, it is possibleto observe that the electrophilic attack has bigger reactivity compared to the nucleophilic and radial attack.

THERMODYNAMIC PROPERTIES

All the thermodynamic data provide helpful information for the study of thermodynamic energies and estimate directions of chemical reactions according to the second law of thermodynamics in thermo chemical field [43]. The thermodynamic parameters such as zero-point vibrational energy, thermal energy, rotational constants, entropy, and dipole moment of title molecule are calculated by B3LYP method using 6-311++G(d,p) and cc-pVDZ basis sets. Scale factors have been recommended [44,45] for an accurate prediction in determining the Zero-Point Vibration Energies (ZPVE) and the entropy, the variations in the ZPVEs seems to be significant Table 10 demonstrates several thermodynamic parameters of the title compound without of results of experimental. The smallest value of ZPVE is 94.35 Kcal/mol obtained at B3LYP/6-311++G(d,p) whereas the biggest value is 94.69 Kcal/mol obtained for B3LYP/cc-pVDZ. The total energies are found to decrease with the increase of the basis set dimension and the change in the Gibbs free energy of title compound at room temperature with different basis set are only marginal. The dipole moment of the molecule was also calculated by B3LYP method with 6-311++G(d,p) and cc-pVDZ basis sets. Dipole moment reflects the molecular charge distribution and is given as a vector in three dimensions. Therefore, it can be used as descriptor to depict the charge movement across the molecule depends on the centers of positive and negative charges. Dipole moments are strictly determined for neutral molecules. For charged systems, its value depends on the choice of origin and molecular orientation. As a result of B3LYP calculations the highest dipole moments were observed for B3LYP/6-311++G(d,p) whereas the smallest one was observed for B3LYP/cc-pVDZ in the title compound.

Table 9 condensed fukui functions calculated by b3lyp/6-311++g(d,p) from the npa and mpa schemes.

Atoms	MPA			NPA		
	f_k^+	f_k^-	f_k^0	f_k^+	f_k^-	f_k^0
N_1	0.0192	-0.0042	0.0076	0.0265	-0.0158	0.0054
C_2	0.1101	-0.0709	0.0196	-0.0143	0.0381	0.0119
S_3	0.2614	0.3109	0.2862	0.3813	0.2244	0.3029
N_4	0.0026	0.0053	0.0042	0.0062	0.0315	0.0189
C_5	-0.0226	0.0474	0.0124	-0.0093	0.1234	0.0571
C_6	0.0133	-0.0334	-0.0101	0.0413	-0.0165	0.0124

C_7	-0.2085	0.0171	-0.0957	-0.0289	0.0088	-0.0101
C_8	0.0627	0.0509	0.0568	0.0502	0.0719	0.0611
C_9	-0.0073	0.0724	0.0326	0.0218	0.1068	0.0643
C_{10}	0.0276	-0.0097	0.0091	0.0559	0.0038	0.0299
C_{11}	0.0131	0.1106	0.0619	0.0203	0.1267	0.0735
O_{12}	0.0971	0.1429	0.1200	0.0984	0.1343	0.1164
H_{13}	0.0434	0.0475	0.0455	0.0496	-0.0061	0.0218
H_{14}	0.0641	0.0436	0.0539	0.0424	0.0197	0.0311
H_{15}	0.2611	-0.0022	0.1295	0.1037	-0.0004	0.0513
H_{16}	0.0267	0.0141	0.0204	0.0467	-0.0026	0.0221
H_{17}	0.0688	0.0745	0.0717	0.0366	0.0321	0.0344
H_{18}	0.0642	0.0751	0.0697	0.0391	0.0355	0.0344
H_{19}	0.0594	0.0665	0.0635	0.0335	0.0334	0.0335
H_{20}	0.0436	0.0413	0.0425	0.0299	0.0207	0.0253

Table 10 The Thermodynamic Parameters Of Btu Along With The Zero Point Energy Calculated By B3lyp Methods

Parameters	B3LYP/6-311++G(d,p)	B3LYP /cc-pVDZ
SCF energy (a.u)	-892.750	-892.641
Zero-point energy (kcal mol-1)	94.3582	94.6921
Rotational constant(GHZ)		
A	1.9880	1.9771
B	0.4095	0.4086
C	0.3395	0.3386
Specific heat (Cv) (cal mol-1 K-1)	35.969	35.614
Translations	2.981	2.981
Rotations	2.981	2.981
Vibrations	30.007	29.652
Entropy (S) (cal mol-1 K-1)	95.383	94.448
Translations	41.471	0
Rotations	31.431	41.471
Vibrations	22.481	31.441
Thermal energy (E) (cal mol-1 K-1)	100.052	100.299
Translations	0.889	0.889
Rotations	0.889	0.889
Vibrations	98.275	98.521
Dipole moment (Debye)		
μx	-1.5647	-1.5032

μy	-0.2444	-0.2378
μz	0	0
μtot	1.5839	1.5034

CONCLUSION

The FT-IR and FT-Raman have been recorded and the detailed vibrational assignment is presented for benzoyl thiourea for the first time. A complete vibrational investigation of the title compound has been performed using FT-IR and Raman spectroscopic techniques. The equilibrium geometries, harmonic frequencies and infrared intensities of the molecule were determined and analyzed by B3LYP with 6-311++G(d,p) basis sets. The simulated FT-IR and Raman spectra of the title compound show good agreement with the observed spectra. The difference between the observed and scaled wave number values of the most of the fundamental is very small. Therefore the assignments with reasonable deviation from the experimental value seem to be correct. This study demonstrates that scaled DFT (B3LYP) calculations are powerful approach for understanding the vibrational spectra of the title molecule. The molecular Gibbs's free energy, the reaction enthalpy and several thermo dynamical parameters were also being found with the ab initio DFT methods. The predicted first hyperpolarizability shows that the molecule might have a reasonably good nonlinear optical (NLO) behaviour.Mulliken atomic charge analysis shows that charge transfer occurring within the molecule.NBO results reflects the charge transfer mainly due to C-O group. The strongest electron donation occurs from σ(N4-H14) to σ*(N4-H16) orbital's. Increased HOMO and LUMO energy gap explains the eventual charge transfer within the molecule which is responsible for the chemical reactivity of the molecule.

REFERENCES

1 Tang L.N, and Wang F.N Electrochemical evaluation of allyl thioureas on copper surface. Corrosion Science. 2008,13: 1156-1160

2 Ziessel R, Bonardi L. Retailleau P, G. Ulrich, Isocyanate-, is othiocyanate-, urea-, and thiourea-substituted borondipyrromethene dyes as fluorescent probes. Org.Chem. 2006, 71: 3093

3 Quraishi M.A, Ansari F.A, D. Jamal. Thiourea derivatives as corrosion inhibitors for mild steel in formic acid .Materials Chemistry and Physics. 2002, 77: 687-690. Sun C W, Zhang X D, Chinese J. Struct. Chem., 2007, 26(2),153-156.

4 Shetty S.D, Shetty P, and Nayak H.V.S, ' The inhibition action of N-(furfuryl)-N'-phenyl thiourea on the corrosion of mild steel in hydrochloric acid medium. Material Letters. 2007, 61: 2347-2349.

5 M.A. Quraishi, F.A. Ansari, D. Jamal. Thiourea derivatives as corrosion inhibitors for mild steel in formic acid .Materials Chemistry and Physics. 2002, 77: 687-690. Hassan H M, J. Serb. Chem. Soc., 1998, 63(2), 117-123.

6 Saeed S, Rashid N, Ali M, Hussain R, Eur. J. Chem., 2010, 1(3), 200-205

7 Z. Zhengyu, D. Dongmei, Mol. J. Struct. (Theochem) 505,247–252 ,(2000)

8 Z. Zhengyu, F. Aiping, D. Dongmei, Int. J. Quant. Chem. 78 ,186–189 ,(2000)

9 Z. Zhengyu, F. Aiping, D. Dongmei, Int. J. Quant. Chem. 78,186–189, (2000)

10 D.C. Young, Computational Chemistry: A Practical Guide for Applying Techniques to Real World Problems (Electronic), John Wiley & Sons Inc, New York,2001.

11 N. Sundaraganesan, S. Ilakiamani, H. Saleem, P.M. Wojciechowski, D. Michalska,Spectrohim. Acta A 61 ,2995–3001,(2005).

12 M.J. Frisch, G.W. Trucks, H.B. Schlegel, G.E. Suzerain, M.A. Robb,J.R. Cheeseman Jr., J.A. Montgomery, T. Vreven, K.N. Kudin, J.C. Burant,J.M. Millam, S.S. Iyengar,J. Tomasi, V. Barone, B. Mennucci, M. Cossi,G. Scalmani, N. Rega, G.A. Petersson, H. Nakatsuji, M. Hada, M. Ehara,K. Toyota, R. Fukuda, J. Hasegawa, M. Ishida, T. Nakajima, Y. Honda, O. Kitao,H. Nakai, M. Klene, X. Li, J.E. Knox, H.P. Hratchian, J.B. Cross, V. Bakken,C. Adamo, J. Jaramillo, R. Gomperts, R.E. Stratmann, O. Yazyev, A.J. Austin,R. Cammi, C. Pomelli, J.W. Ochterski, P.Y. Ayala, K. Morokuma, G.A. Voth,P. Salvador, J.J. Dannenberg, V.G. Zakrzewski, S. Dapprich, A.D. Daniels,M.C. Strain, O. Farkas, D.K. Malick, A.D. Rabuck, K. Raghavachari, J.B. Foresman,J.V. Ortiz, Q. Cui, A.G. Baboul, S. Clifford, J. Cioslowski, B. Stefanov, G. Liu,A. Liashenko, P. Piskorz, I. Komaromi, R.L. Martin, D.J. Fox, T. Keith,M.A. Al-Laham, C.Y. Peng, A. Nanayakkara, M. Challacombe, P.M.W. Gill,B. Johnson, W.Chen, M.W. Wong, C. Gonzalez, J.A. Pople, Gaussian 03,Revision A.I, Gaussian, Inc, Pittsburgh, PA, 2003.

13 P.C.HAriharan,J.A.Pople,Theo.Chim.Acta, ,28,213(1973).

14 P.C.HAriharan,J.A.Pople,Mol.Phys, ,27,209(1974).

15 A.D.Becke,J.Chem.Phys, ,98,5648(1993).

16 A.E.Reed,L.A.Curtiss,F.Weinhold,Chem.Rev.,88,899,(1988).

17 E.D.Glendening,A.E.Reed,J.E.Carpenter,F.Weinhold,J Am Chem Soc, ,120,12051(1998)
18 Usharani,M.karabacak,O.Tandriverdi,M.kurt,N.Sundaraganesan, Spectrochim Acta, A,92 ,67– 77 ,(2012).
19 V.K. Rastogi, M.A. Palafox, R.P. Tanwar, L. Mittal, Spectrochim. Acta A 58, 1987–2004, (2002).
20 M. Silverstein, G.C. Basseler, C. Morill, Spectrometric Identification ofOrganic Compounds, Wiley, New York, (1981).
21 L.J. Bellamy, The Infrared Spectra of Complex Molecules, 3rd ed., Wiley, NewYork, (1975).

22 M. Karabacak, Z. Cinar, M. Kurt, S. Sudha, N. Sundaraganesan Spectrochimica Acta Part A 85 ,179– 189 ,(2012).
23 G. Socrates, Infrared Characteristic Group frequencies, Wiley-Interscience Publication,New York, (1980).
24 G. Varsanyi, Assignments of Vibrational Spectra of Seven Hundred Benzene Derivatives, vols. 1–2, Adam Hilger, (1974).
25 V. Krishnakumar, V. Balachandran, Spectrochim. Acta A ,61, 1001–1006,(2005).

26 D.N. Sathyanarayana, Vibrational Spectroscopy, Theory and Applications, New Age International Publishers, New Delhi, 2004.

27 M. Snehalatha, C. Ravi kumar, I. Hubert Joe, N. Sekar, V.S. Jayakumar, Spectrochim. Acta A, 72 ,654(2009)

28 C. James, A. Amal Raj, R. Reghunathan, I.H. Joe, V.S. Jayakumar, J. Raman Spectrosc, , 37,138,(2006).

29 J. Liu, Z. Chen, S. Yuan, J. Zhejiang, Univ. Sci., B 6,584, (2005).

30 Atalay, D. Avil, A. Basaoglu, Struct. Chem. 19, 239,(2008).

31 T. Vijayakumar, I. Hubertjoe, C.P.R. Nair, V.S. Jaya Kumar, Chem. Phys. 343 83–89,(2008).

32 I. Sidir, Y.G. Sidir, M. Kumalar, E. Tasal, J. Mol. Struct. 134,964,(2010).

33. K. Jug, Z.B. Maksic, in: Z.B. Maksic (Ed.),Theoretical Model of Chemical Bonding, Part 3, Springer, Berlin,, 29, 233,(1991).

34. S. Fliszar, Charge Distributions and Chemical Effects, Springer,New York,(1983).

35. L. Xiao-Hong, et al., Comput. Theor. Chem., 2 ,969, (2011).

36 S. Sebastin, N. Sundaraganesan, Spectrochim. Acta A 75 ,941-952,(2010).

37 E. Scrocco, J. Tomasi, Adv. Quantum Chem. 11,115,(1979)

38 C.R. Zhang, H.S. Chen, G.H. Wang, Chem. Res. Chin., , U 20 ,640,(2004).

39 Y. Sun, X. Chen, L. Sun, X. Guo, W. Lu, Chem. Phys. Lett., 38, 397,(2003).

40 O. Christiansen, J. Gauss, J.F. Stanton, Chem. Phys. Lett., 147,305, (1999).

41 P. Kolandaivel, G. Praveen, and P. Selvarengan, J. Chem.Sci 117(5),591(2005)

42 R.K. Roy, K. Hirao, S. Krishnamurthy, and S. Pal, J. Chem. Phys.,115,2901 (2001)

43 R. Zhang, B. Dub, G. Sun, Y. Sun, Spectrochim. Acta A 75 ,1115–1124, (2010).

44 M. Alcolea Palafox, Int. J. Quantum Chem. 77,661–684, (2000).

45. R.Desiderato, J.C.Terry, G.R.Freeman, Acta Crystallogr.Sect.B 27,2443,(1971).